



# Computer aided simulation and performance evaluation of additive manufacturing technology for component parts manufacturing

Ilesanmi Daniyan<sup>1</sup> · Khumbulani Mpofo<sup>1</sup> · Lanre Daniyan<sup>2</sup> · Festus Fameso<sup>3</sup> · Moses Oyesola<sup>1</sup>

Received: 14 November 2019 / Accepted: 16 April 2020 / Published online: 28 April 2020  
© Springer-Verlag London Ltd., part of Springer Nature 2020

## Abstract

Additive manufacturing technology involving the deposition of materials in successive layers provides a realistic possibility for easy and quick production of 3D objects on demand. This work involves the computer-aided simulation and performance evaluation of an additive manufacturing technology. The mechanical design, modelling and simulation of the internal accessory of a railcar were carried out with the aid of the ABAQUS® 2016 while the physical experimentations were carried out via the fused deposition modelling (FDM) method using three different 3D printing materials, namely acrylonitrile butadiene styrene (ABS) plastic, epoxy resin and polytetrafluoroethylene. An additive manufacturing system which essentially comprises the mechanical part having the stepper motor, micro-switch and extruder, and the electronics board having MELZI V2.0, a DIY shield board, USB to serial converter and Arduino micro controller was used for the product manufacturing. The analysis of the results gotten indicates that the three materials possess excellent mechanical properties which make them suitable for the service requirements. This work will assist manufacturers in their quest for innovativeness in product development as well as reduction in the manufacturing lead time and cost.

**Keywords** Additive manufacturing · Computer-aided simulation · FDM · Micro controller · Railcar

## 1 Introduction

The quest for a greener technology that is a production process which is sustainable in terms of reduction in waste generation and energy consumption has triggered recent innovation and advances in the area of additive manufacturing (AM) technology. The manufacturing technology has continued to gain widespread attention in the manufacturing industry due to its suitability for rapid production of components with a near net shape [1–3]. In addition, the need to reduce the manufacturing lead time and cost with the development of high-quality

products with repeatability are challenges that require appreciable solution in the industry. This has prompted manufacturers to embrace emerging materials and technologies geared towards product innovation. The railcar manufacturers are increasingly testing the potentials of the additive manufacturing technology to break the creative barriers within the three major areas, namely product innovation, rapid high-volume direct manufacturing and energy efficiency. The complexity and intersecting technologies driving the Fourth Industrial Revolution and the breadth of their impact necessitate the development of innovative approaches to implement and diffuse the current and emerging technologies for railcar development. In response to the increasing dynamics of the manufacturing and business landscape in terms of product development, product customization, market competition, globalization amongst others, the quick and efficient production of quality products is critical to the success of the manufacturing industries. The additive manufacturing technology offers a realistic possibility for rapid product development in this regard [4–7]. The 3D printing also known as the rapid prototyping is one of the various forms additive manufacturing technology whereby a 3D object is created through successive deposition of materials in layers [8–10].

---

✉ Ilesanmi Daniyan  
afolabiilesanmi@yahoo.com

<sup>1</sup> Department of Industrial Engineering, Tshwane University of Technology, Pretoria 0001, South Africa

<sup>2</sup> Centre for Basic Space Science, University of Nigeria, Nsukka, Nigeria

<sup>3</sup> Department of Mechanical & Automation Engineering, Tshwane University of Technology, Pretoria 0001, South Africa

The merits lie in the freedom of geometry, development of a cost-effective technology and the realistic possibility for easy and quick production of an object with a near net shape on demand. The use of the 3D production technology in manufacturing is often rapid and cost effective which in the real sense has the potential to open the door for innovative production. Over the years, various additive manufacturing technologies have been employed for the development of specialized parts, components or products, medical equipment, teaching aids and sensors etc. [11]. In the automobile and rail manufacturing, it is suitable for developing components with complex geometries, tools and other parts or sub-assemblies. The technology can significantly improve the life cycle of products from the design to the end of life phases. If the AM technology is adequately deployed, it has the capacity to transform the manufacturing and business landscape. This is due to its flexibility and versatility in the production of complex geometries which are usually difficult to produce traditionally. The AM process eliminates the use of special tooling, jigs and fixturing elements which makes it a relatively simple manufacturing process. The AM process is highly conservative and environmentally friendly and also promotes the concept of circular economy with the tendency to reuse some of the production materials [12]. When the manufacturing process conditions are carefully planned, it has the capacity to produce objects with near net shape, thereby eliminating the need for expensive post processing. This will also save the manufacturing lead time considerably, thus, making the process time and cost effective. The AM technology for product development boast of manufacturing flexibility, product customization, product variability, time and cost effectiveness as well as effective production mix [13]. For the manufacturing industries to fully explore the potentials of the AM technology, there is need for an effective process design which will integrate the computer aided design into the manufacturing phase for product development. As part of an emerging revolution in the railcar manufacturing industry, this work considers the integration of the computer-aided simulation approach and shop floor manufacturing for the rapid production of railcar components via the additive manufacturing technology. The work which integrates the computer-aided design and simulation phase with the manufacturing phase offers realistic possibility for effective monitoring and control during the production process. This is because the texture, composition and the distribution of the starting materials as well as the optimum combination of the process parameters are critical to the overall success of the manufacturing process. The deviations beyond the permissible limit will translate into the need for expensive post processing or rework. Many researchers have reported on various approaches to enhance the additive manufacturing process for product development. For instance, Laplulme et al. [14] reported on an open-source, 3D printer factory capable of self-replicating for small medium

enterprises. The study showed that the 3D printing business model is sustainable and can offer cost effective products while maintaining healthy profit margins. Valkenaers et al. [15] reported on a novel approach to additive manufacturing involving screw extrusion 3D printing. The research findings indicate that the approach is highly sustainable in terms of energy, material and cost effectiveness. In a bid to ensure that components developed additively meet their required service and functional requirements, Gurralla and Regalla [16] reported on the part strength evolution with bonding between filaments in the fused deposition modelling (FDM). The study investigated the coalescence of filaments and how it enhances the strength of the final product. Similarly, Wang et al. [17] developed a novel approach to improve the mechanical properties of parts fabricated by the FDM technique. The research findings from these works indicated that the process parameters are critical factors which determine the integrity of the final product. In the light of this, Chaidas et al. [18] studied the effect of temperature variation on the surface roughness of component parts manufactured via the fused filament fabrication (FFF) while Lužanin et al. [19] studied the effect of extrusion speed and temperature on the surface roughness of components produced using the FDM technique. The findings from the works of Chaidas et al. [18] and Lužanin et al. [19] indicated that temperature and speed of printing are critical factors as they promote the homogenisation and fusion of the constituent materials in order to obtain a final product with high surface integrity. However, when the optimum values of the critical factors are exceeded, the process becomes less sustainable. Hence, the need for effective process monitoring and control in order to keep the operating conditions within the optimum range.

Although many works have been reported on the development and application of 3D printing technology, its application in railcar manufacturing using acrylonitrile butadiene styrene (ABS) plastic, epoxy resin and polytetrafluoroethylene has not been sufficiently reported by the existing literature. In addition, the integration of the computer-aided modelling and simulation phase with the manufacturing phase validated by physical experimentations for the production of railcar accessories has not been widely reported. Hence, the aim of this work is to integrate the computer-aided modelling and simulation approach and shop floor manufacturing for the rapid production of railcar components via the additive manufacturing technology. The validation of the numerical approach employed will be done with the physical experimentations involving the use of acrylonitrile butadiene styrene (ABS) plastic, epoxy resin and polytetrafluoroethylene for the production of railcar accessories. The findings of this research will assist manufacturers most especially those in the rail sector in exploring the prospects of additive manufacturing (AM) in order to strike the right balance among competing factors: cost effectiveness, high-volume direct manufacturing, product

development cycle time and increased product performance. Furthermore, it will also assist manufacturers in their quest for innovativeness in product development as well as reduction in the manufacturing lead time and cost.

## 2 Methodology

The work involves the computer-aided simulation and performance evaluation of an additive manufacturing technology that is suitable for producing the internal and external accessories of a railcar from a CAD file. A host software was employed which controls the movement of the 3D printer, slice the .STL (Stereolithography) files format and generates the G Codes (set of instruction). It uses the concept of modularity to implement the control of the 3D printer system. The 3D printer has the following modules: *repetier* host software, heat bed, extruder, motor and the main control. Each of these modules is controlled by an independent microcontroller which is interconnected with the module of the main control, for effective coordination of the tasks of the 3D printer system. A Computer-aided design (CAD) file is created with the aid of a 3D modelling program, which creates and sends the file to the 3D printer. The host software slices the design into different layers ranging from hundreds to thousands in a horizontal layer. The sliced layers will thereafter be printed on the top of each other until the 3D object is produced. The print table is the platform which provides the basic support for manufacturing objects layer by layer upon which the objects for printing are situated. The extruder is one of the most important parts of a 3D printer usually employed for material and ink deposition during printing. The movement of extruder in various dimensions creates the 3D print. For printing a 3D object, the extruder has to access X, Y and Z coordinates depending on the specification of the printer required for various applications. The type of 3D printer investigated is based on fused deposition modelling (FDM) technology because it is the most commonly used in the ranks of the 3D printers. Figure 1 shows the frame work for the developed additive manufacturing technology which integrates the computer-aided modelling and simulation phase with the shop floor manufacturing. The framework incorporates all the requirements (service, design and material requirements) for the additive manufacturing of components. This is followed by the preliminary design and the application of the computer-aided design modelling and simulation tools to determine the feasibility of the proposed solution before proceeding to the final design stage. If the requirements are met considerably, the final design will be made for the production of the component parts. Otherwise, adjustments will be required in an iterative process until such requirements are met. The framework integrates the CAD phase with the manufacturing phase for additive manufacturing since the production process is usually initiated with the

creation of a 3D model of the parts to be produced. At the CAD design phase, the creation of the 3D model of the object to be produced via a CAD software is followed by the geometric specifications of the object as well as the discretization of the solid model into different shapes using the .STL extension. The created .STL files are converted into the G-codes (instructions) for component part manufacturing. This implies that the quality and the degree of conformity of the final product are determined right from the CAD phase. Hence, the need for the development of an efficient process design for proper analysis, modelling, simulation and optimization of the different configurations of the 3D model that will meet the stated requirements.

### 2.1 Uploading the bootloader with an AVR programmer

The chip usually comes blank and the bootloader was burnt onto the chip with the aid of the AVR programmer. The Arduino IDE software was downloaded while the AVR programmer was connected to the PC via the USB. The Melzi board was powered by the USB and the programmer was also connected to the Melzi via the Serial Peripheral Interface (SPI) pins. When the Arduino IDE was opened, the Arduino was turned “ON”. This was followed by the selection of the AVR Programmer type as well as the burn bootloader.

### 2.2 Firmware upload

The Firmware Melzi board of the system comprises two ports for each of the three end stops, and the three stepper motors in the X, Y and Z directions, respectively, as well as two ports each for the hotbed, fan, extruder and the thermistor system. The board is powered by a 12 V 25 A source and also has a port for the TF card, USB and ISP programmer. In order to upload the firmware, both the Arduino and the Melzi board were connected to a PC. This is followed by the opening of the Arduino IDE, card selection and the turning on of the arduino as well its selection as the ISP.

### 2.3 Melzi Arduino pin numbers

The pin numbers of the Melzi Arduino board are as follows:

```
#define X_STEP_PIN 15
#define X_DIR_PIN 21
#define X_MIN_PIN 18
#define Y_STEP_PIN 22
#define Y_DIR_PIN 23
#define Y_MIN_PIN 19
#define Z_STEP_PIN 3
#define Z_DIR_PIN 2
#define Z_MIN_PIN 20
```

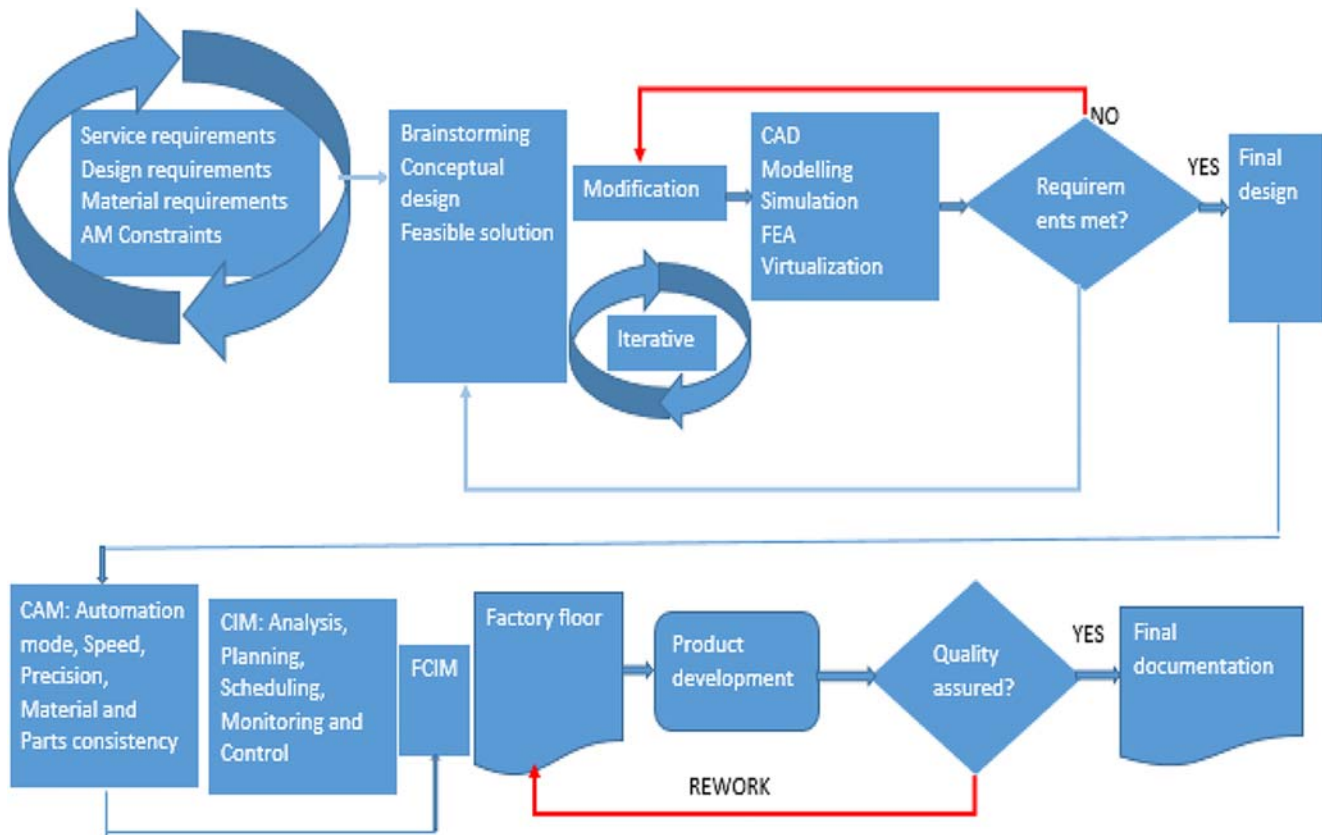


Fig. 1 The frame work for the developed additive manufacturing technology [20]

```

#define E0_STEP_PIN 1
#define E0_DIR_PIN 0
#define LED_PIN 27
#define FAN_PIN 4
#define HEATER_0_PIN 13 // extruder
#define HEATER_BED_PIN 10 // bed (change to 12 for
breakout pin on header)
#define X_ENABLE_PIN 14
#define Y_ENABLE_PIN 14
#define Z_ENABLE_PIN 26
#define E0_ENABLE_PIN 14
#define TEMP_0_PIN 7 // Analogue pin
#define TEMP_BED_PIN 6 // Analogue pin
#define SDSS 31
#define SLAVE_CLOCK 16

```

#### 2.4 Phase III software part (Repetier host)

The Repetier host is the software employed in the control of the axes of the 3D printer and slicing of the .STL files. After saving a CAD file in the .STL file format, it is then loaded in the Repetier host firmware which slices the models, thereby generating G-code (instructions) which was used for the printing operation.

#### 2.5 System's energy requirement

Equation 1 presents the sum of the current needed for the printing process.

$$I_t = I_f + I_m + I_h \quad (1)$$

where  $I_t$  is the total current drawn for part processing during the printing operation (Amp),  $I_f$  is the current consumed by the fans (Amp),  $I_m$  is the current used by the motors (Amp) and  $I_h$  is the current used by the heater (Amp).

The length of traversal ( $L$ ) which measures the distance moved by the nozzle during the execution of the command given by the G-code file is expressed as Eq. 2; thus,

$$L = \sqrt{(X_i - X_{i-1})^2 + (Y_i - Y_{i-1})^2} \quad (2)$$

where  $X_i$  denotes the  $i^{\text{th}}$  command given by the G-code,  $X_i$  and  $Y$  are the coordinates of the instruction  $X_{i-1}$ .

The power required ( $P$ ) for the printing process expressed as Eq. 3.

$$P = I_t \times V \quad (3)$$

where  $V$  is the supplied voltage (120 V) with a variation of  $\pm 0.5$  V.

The corresponding energy consumed is the product of the power required and the printing time expressed as Eqs. 4 and 5 while Eqs. 6 and 8 present the overall energy equation for the printing process which can be used for the development of an energy model for the 3D printing process.

$$E = P \times T \quad (4)$$

where  $T$  is the printing time (s)

$$E = I_t \times V \times T \quad (5)$$

$$E = \sum_{i=1}^T E_i = \sum_{i=1}^T I_t \times V \times T \quad (6)$$

The printing time is a function of the length of traversal ( $L$ ) and the speed of printing ( $s$ ) expressed as Eq. 7.

$$T = \frac{L}{s} \quad (7)$$

where  $L$  is the length of traversal ( $m$ ) and  $s$  the speed of printing ( $m/s$ ).

Hence, Eq. 6 is modified to obtain Eq. 8.

$$E = \sum_{i=1}^T E_i = \sum_{i=1}^T \frac{I_t \times V \times L}{s} \quad (8)$$

## 2.6 The materials employed

Three different 3D printing materials, namely acrylonitrile butadiene styrene (ABS) plastic, epoxy resin and Teflon, were employed for the product development. ABS is a lightweight thermoplastic polymer with good mechanical properties such as high strength, stiffness and toughness. It is highly flexible, recyclable, cost effective, flame retardant, with excellent resistance to heat and corrosion. It is suitable for the manufacture of automobile and railcar parts, because its rheological properties often promote the development of products with high degree of surface finish. In situations where post processing is required, 3D printed models from ABS can be post processed without compromising the integrity of the material. It can also come in different colour varieties in order to meet the aesthetic requirements and its excellent resistance to heat and corrosion makes it suitable for certain applications where other materials might fail. The demerits being the production of hot toxic plastic fumes during printing, and the ease of deformation when not printed on a hot surface. Its high glass transition temperature can also cause the product to retain internal thermal stresses which can promote the shrinkage of the final product after manufacturing. On the other hand, the epoxy resin is tough, cost-effective, has good mechanical properties such as high strength, high stiffness, high impact resistance, and it is suitable for the production of prints with good surface finish, high resolution and precision. The

limitations lie in its low flammability resistance and high temperature requirement during printing. In addition, polytetrafluoroethylene (PTFE) otherwise known as Teflon is a non-stick, dimensionally stable high temperature, chemical resistant 3D printing material which offer sustainable manufacturing solution on a range of design applications. It has good properties such as good heat and chemical resistance. It is highly recyclable with high moisture absorption ability. The limitations lie in the cost and its non-suitability for making complex geometries [21, 22].

## 2.7 The numerical modelling and simulation

The models of the railcar accessory (fire extinguishing mounts) as shown in Fig. 4 were subjected to structural analyses via the numerical simulations. The commercial finite element modelling and simulation software ABAQUS® CAE was used for simulation in order to determine the behaviour of the models when subjected to the required loading conditions. Hence, the behaviour of the models of the three different 3D printing materials employed, acrylonitrile butadiene styrene (ABS) plastic, epoxy resin and Teflon, to loading conditions were investigated and compared. This is necessary because the efficiency of printing and the integrity of the printed parts are functions of the properties, micro structure and chemistry of the materials employed. For instance, the temperature of the extruder which is necessary for part printing can be significantly influenced by the melting temperature of the material. In addition, the coefficient of thermal expansion can also determine the magnitude of the thermal stresses developed within the material during the printing process which can significantly affect the bed adhesion. It is assumed that the loading is static and that the materials are subjected to the same loading and service requirements.

Table 1 shows the properties of the three materials employed in the geometric and material modelling of the product in the simulation code. The comparative analyses were carried out based on the results of the simulations obtained.

The extrusion temperature is the temperature of the heater block at the hot end of the printer while the bed temperature is the temperature of the build plate surface on which the printed materials is placed.

The railcar accessory was designed to be a fire extinguisher mount in a railcar and was thus subjected to loads and boundary conditions that mimic the scenario of its actual usage. The geometric model of the accessory as well as the loading and boundary condition definitions on the Complete Abaqus Environment (CAE) are shown in Fig. 2 a and b. The Abaqus implicit module was employed because the implicit dynamic simulations can be applied to structural analysis with non-linear analysis; hence, it was used for the structural non-linear analysis of the 3D printed components. The implicit

**Table 1** Properties of 3D printing materials [21, 22]

Properties	ABS plastic	Epoxy resin	Teflon
Density (kg/m <sup>3</sup> )	936	1683	2275
Young's modulus (GPa)	2.34	10.5	2.5
Yield strength (MPa)	48	85	41
Thermal conductivity W/(m.°C)	0.12	0.43	0.24
Specific heat (K <sup>-1</sup> )	500	795	264
Extrusion temperature (°C)	220–240	270–315	230–255
Bed temperature (°C)	80–110	90–120	55–70
Glass temperature	105–110	145–150	70–78
Coefficient of thermal expansion (µm/m. °C)	68–110	50–70	60–92

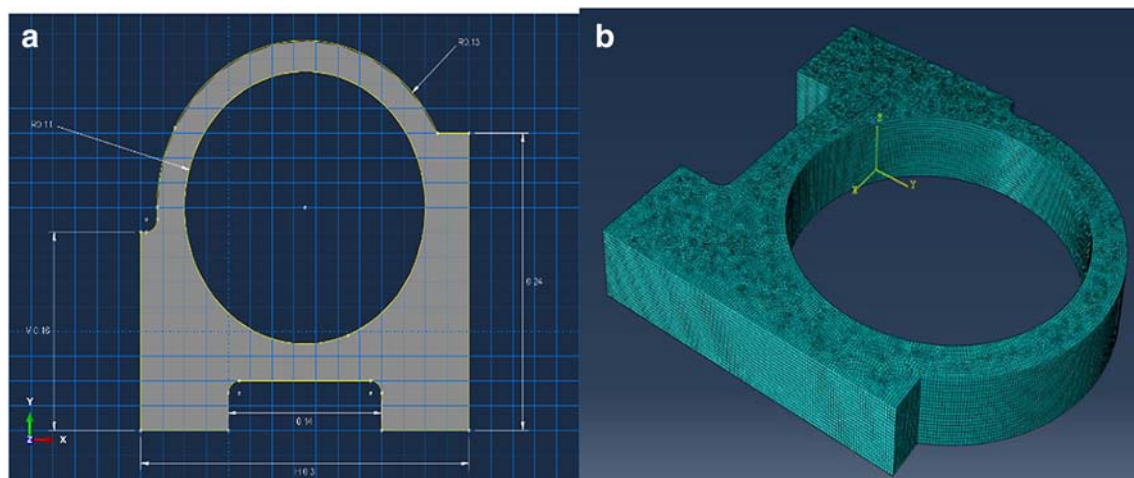
module has a suitable integrator for the formulation and analysis of a non-linear behaviour. It is an iterative process with time increment adjustments until the solution finally converges. Following the meshing of the assembly into finite elements, it was subjected to convergence simulation runs with mesh refinement feature employed for the ease of convergence. An average mesh size of 0.8 mm which falls within the seed size stability convergence zone was employed, in order to strike the right balance among the computational costs, efficiency and accuracy in contrast with other mesh sizes within the convergence band.

The 3D part was drafted and meshed with standard 3D stress analysis, 8-node linear brick finite elements, with reduced integration and default hourglass control.

The meshed parts were imposed with encastre mechanical boundary conditions at the fixed end and a load of 300 N (about 30 kg) which is more than the average weight of an industrial sized fire-extinguisher was imposed on the inner channels of the accessory which will hold the extinguisher mount in the right position. The loading of the fire extinguisher mount is shown in Fig. 3 a and b.

## 2.8 The physical experimentation

The printing method employed was the fused deposition modelling (FDM). The process involves the heating of the thermoplastic to the melting temperature and the subsequent extrusion of the molten thermoplastic as well as the material's deposition and binding layer by layer. The process is relatively simple, cost and time effective and permits the development of products with complex geometry as well as the deposition of multi-material in layers though with the limitations of low repeatability, as well as high operating temperatures [23, 24]. The printing process is depicted by Fig. 4. The optimum values of the process parameters selected are as follows: print speed (75 mm/s), nozzle diameter (0.15 mm), thickness of layers (0.10 mm), extrusion temperature (255 °C), bed temperature (87.5 °C) and percent of material in part volume (15%). The selection of the range of the process parameters namely print speed, nozzle diameter and thickness of layer was informed based on a similar work reported by Lužanin et al. [19] while the extrusion and bed temperatures were obtained by finding the average values of the optimum range for the three materials investigated in this study (Table 1). The

**Fig. 2** a, b The 3D geometric model of the accessory

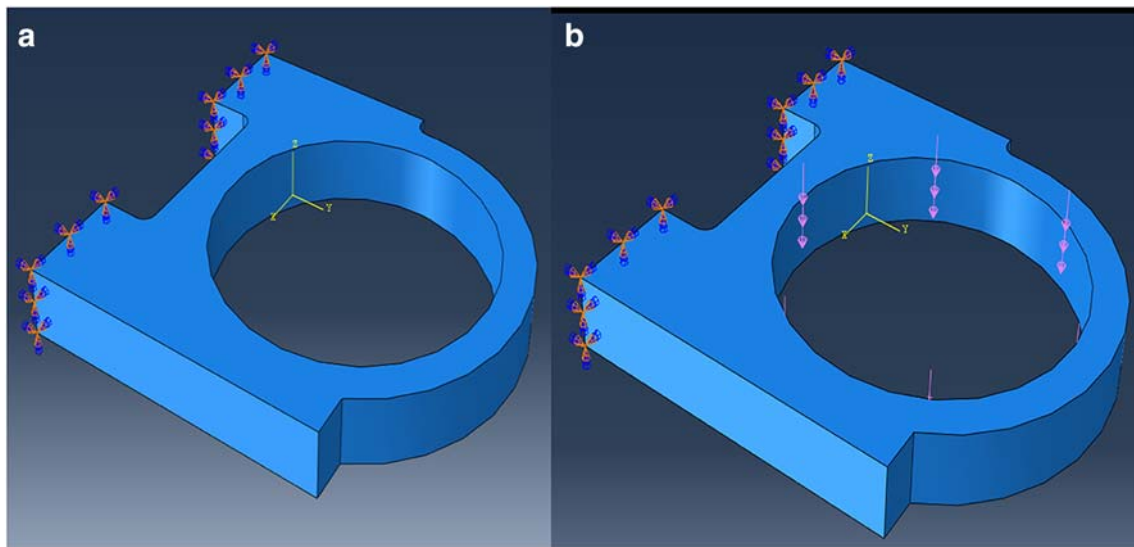


**Fig. 3** a, b Loading and boundary condition definitions on the CAE

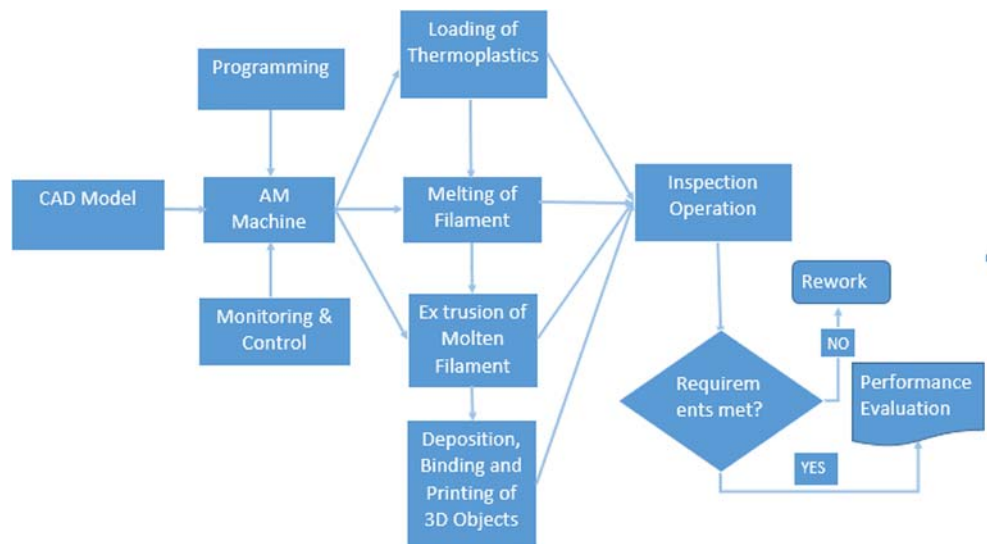
files of the 3D objects are first created with the computer-aided design (CAD) software as CAD files and then converted to the .STL files; thereafter, the .STL files were imported into the host software (Repetier) which slices STL files into the different layers in order to determine the way in which the extruder would build each of the layer. This generates some set of instructions (G-code) which is transmitted to the machine for the execution printing process. The computer program controls the nozzle and base, which converts the object’s dimension into the X, Y and Z, coordinates for printing. The filaments of the three thermoplastic materials (acrylonitrile butadiene styrene (ABS) plastic, epoxy resin and polytetrafluoroethylene) were unwound from a coil and loaded into the extrusion nozzle. At the extrusion nozzle, the filaments were heated to the molten temperature followed by subsequent extrusion through the nozzle to the base. The

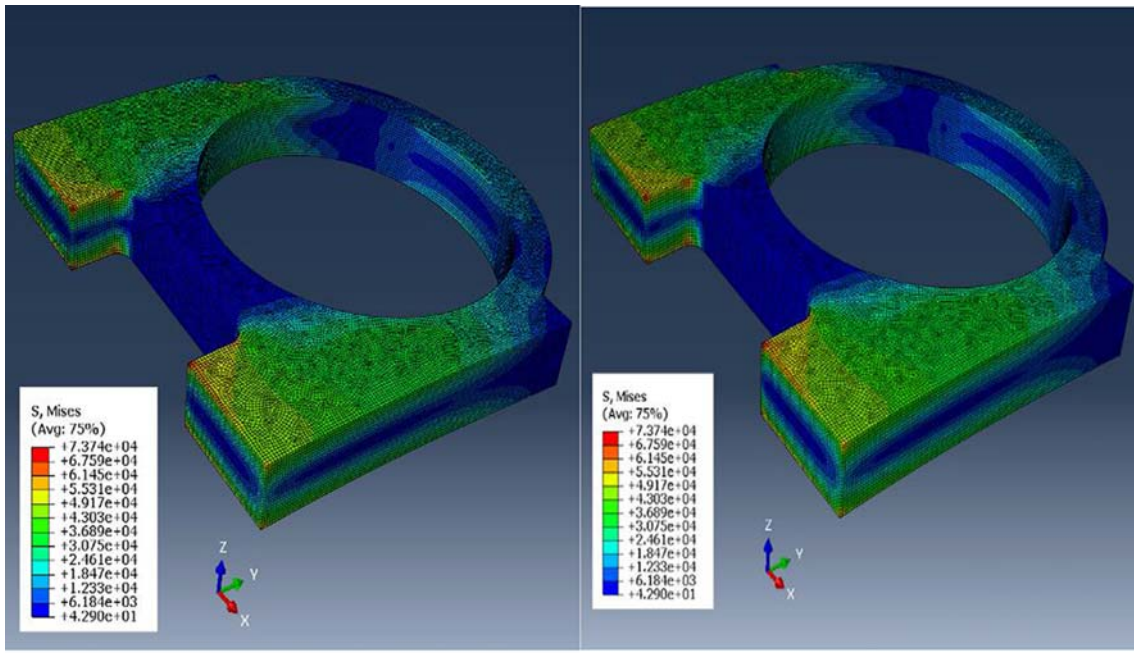
horizontal and vertical movement of the extrusion nozzle over the extruded product draws some objects into the base. The product is extruded layer by layer at the base to create a three-dimensional object. As soon as one layer is finished, the nozzle moves in the Z-direction to the next layer. The melted thin layer cools and hardens, thus binding successive layers together to form a 3D printed part.

### 3 Results and discussion

The distribution of stresses in the material during loading is presented in Fig. 5 a–d. The Von Mises stresses as presented are essentially the resultant of all the normal and shear stress impact on the modelled part. It presents information on the isotropic response of the material, and whether it will yield

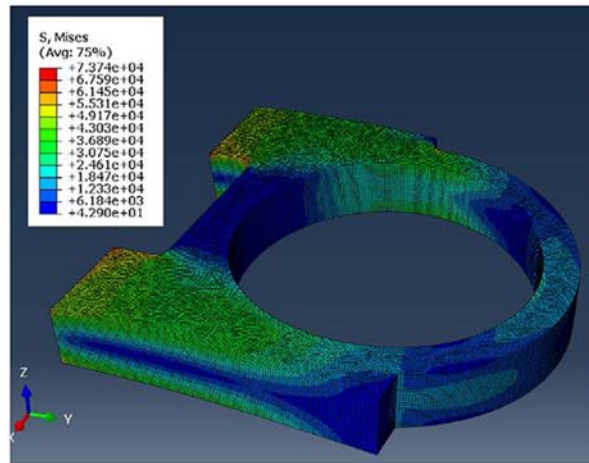
**Fig. 4** The schematics of the printing process



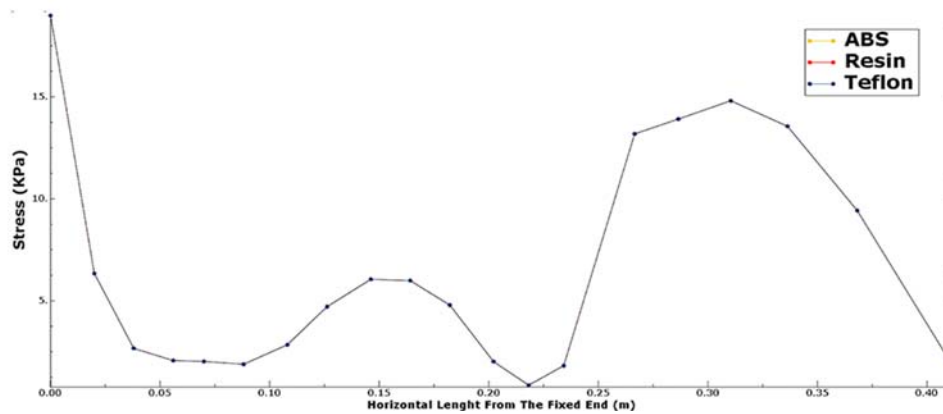


(a) ABS

(b) Resin



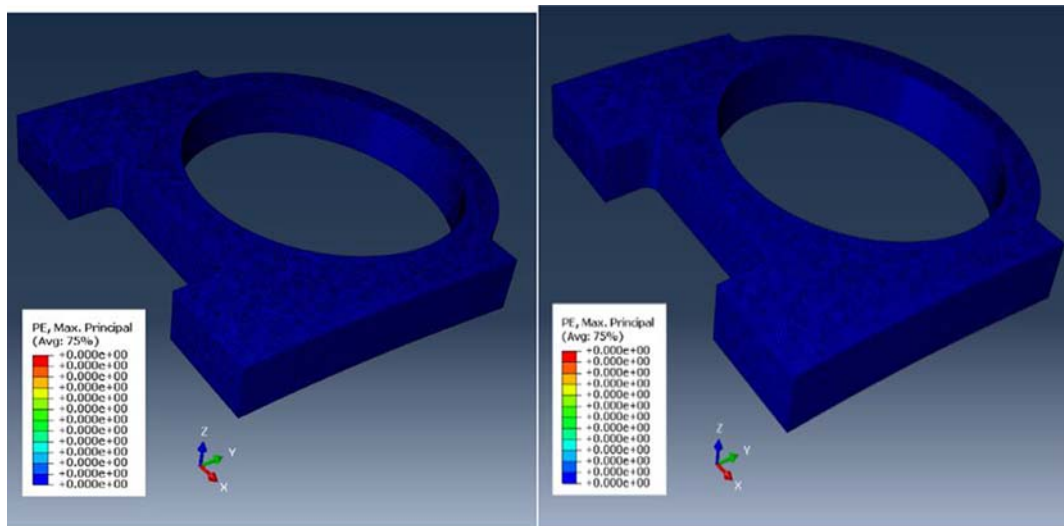
(c) Teflon



(d) Graphical representation of the stress distribution across the horizontal length to the accessory.

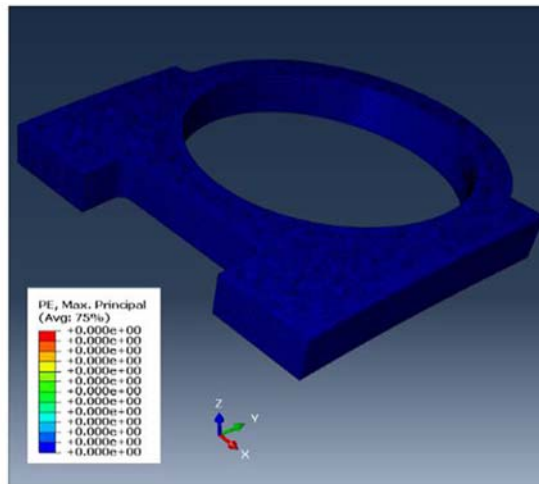
Fig. 5 a ABS, b Resin, c Teflon, d graphical representation of the stress distribution across the horizontal length to the accessory



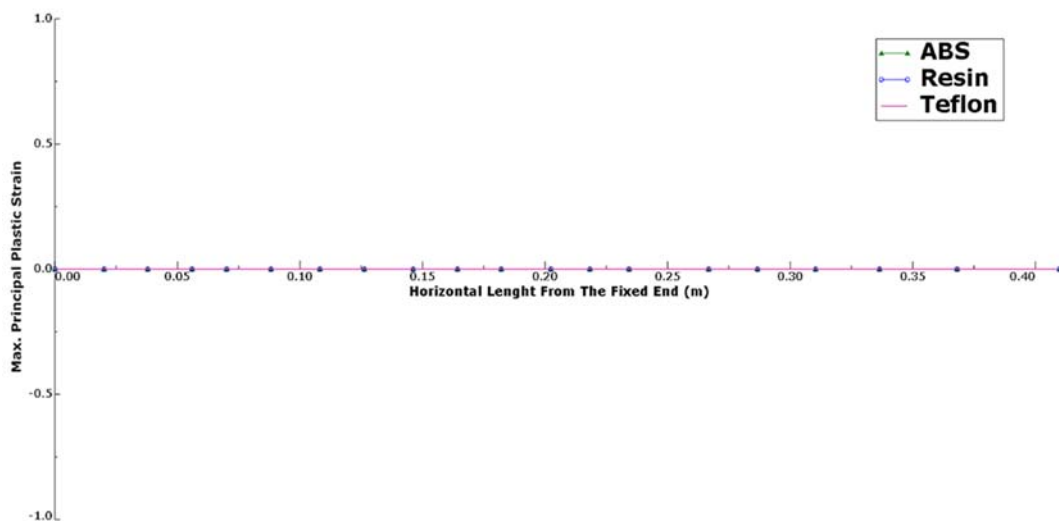


(a) ABS

(b) Resin

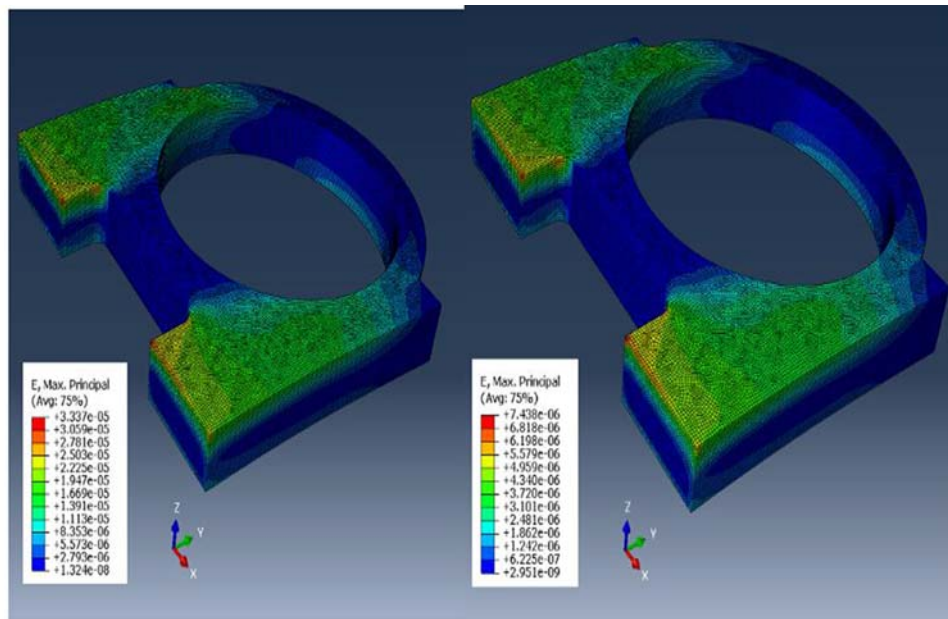


(c) Teflon



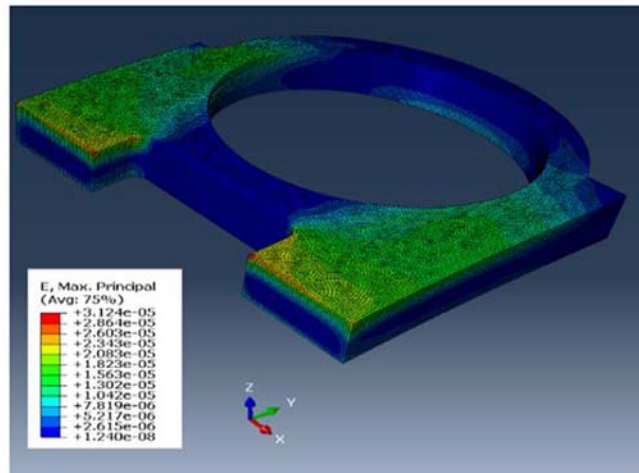
(d) Graphical representation of the max principal plastic strain distribution across the horizontal length of the accessory.

Fig. 6 a ABS, b Resin, c Teflon, d graphical representation of the max principal plastic strain distribution across the horizontal length of the accessory

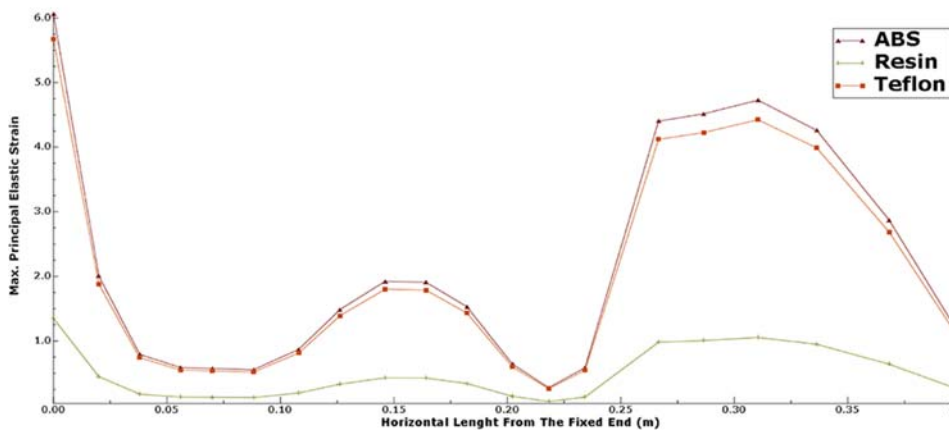


(a) ABS

(b) Resin

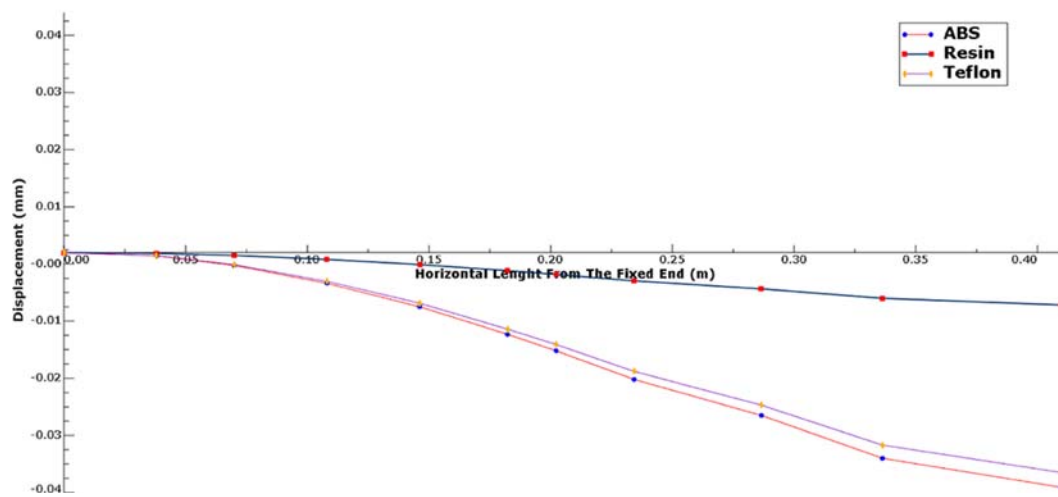
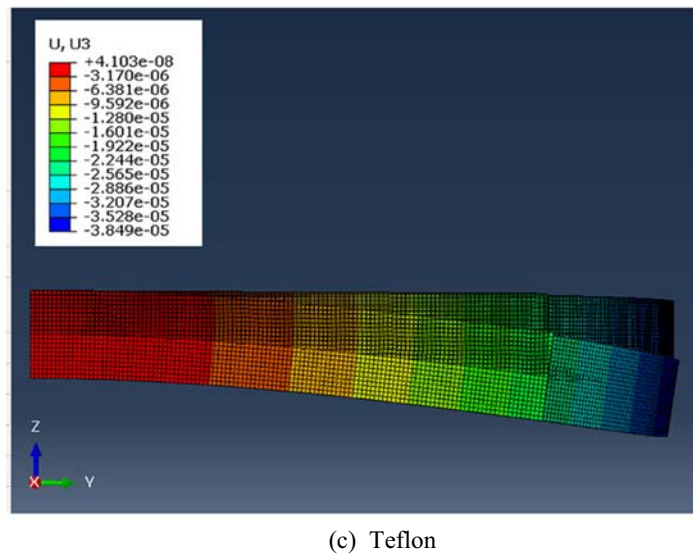
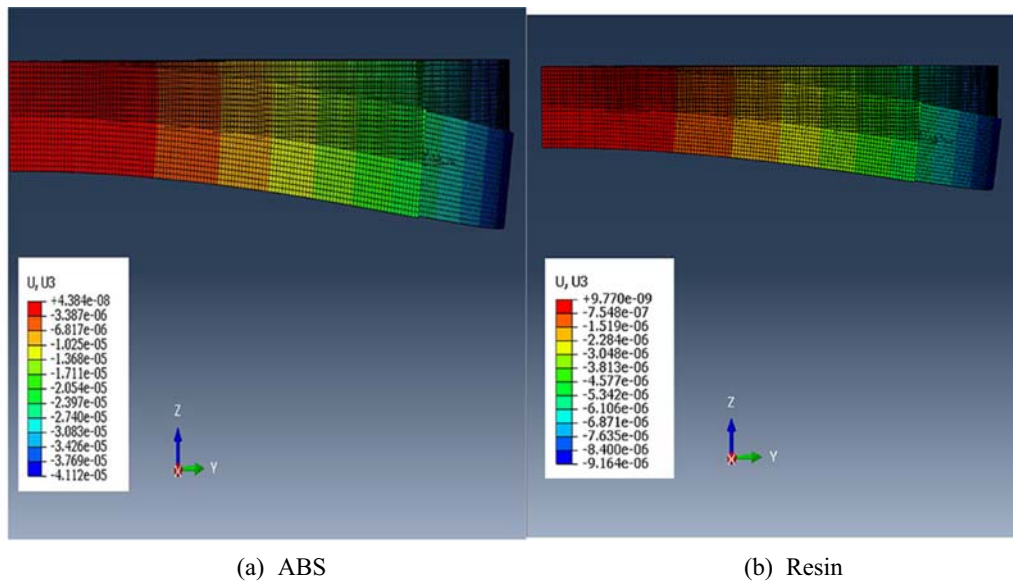


(c) Teflon



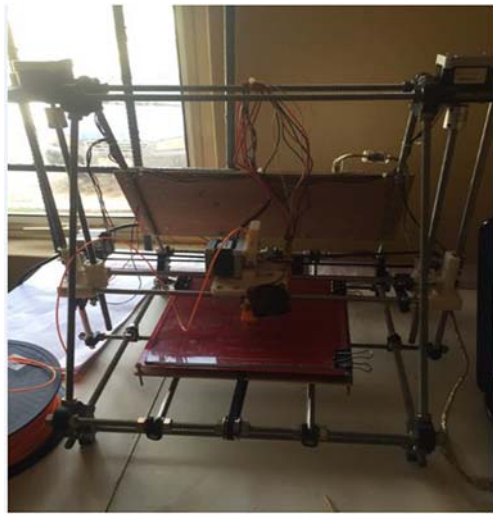
(d) Graphical representation of the maximum principal elastic strain distribution across the horizontal length of the accessory.

Fig. 7 a ABS, b Resin, c Teflon, d graphical representation of the maximum principal elastic strain distribution across the horizontal length of the accessory



(d) Graphical representation of the downward displacement across the horizontal length of the accessory.

Fig. 8 a ABS, b Resin, c Teflon, d graphical representation of the downward displacement across the horizontal length of the accessory



**Fig. 9** The 3D printer

when subjected to complex loading conditions. The pictorial representation shows a similarity in the stress profile in the three different materials considered after loading. This similarity is corroborated by the stress against horizontal distance (y-axis in this case) graph where the values correspond perfectly. This thus gives an indication of how the stresses will be distributed in the final product, given the same magnitude of load, irrespective of the material it is made of. The maximum stress recorded for the three materials was 73.74 kPa, which is much less than the yield strength of any of the three materials under consideration (between 41 and 85 MPa). This indicates that the product from any of these three materials will not fail under the conditions of static loading and will more likely hold more weights, whose values are greater than the current design weight. The similarities in the stress profiles coupled with the fact that the maximum stresses are lower than the yield strength of the three materials indicate the three materials possess excellent strength for the required service condition.



**Fig. 10** The 3D printed models (fire extinguisher mounts)

The maximum principal plastic strain result is shown in Fig. 6a–d. This also lends some credence to fact that the structural integrity is guaranteed for the design load. There is zero plastic shear strain in the model of the developed product for all the materials considered. The plastic strain is a measure of the strain when the component is subjected to stresses beyond the yield point. The results obtained indicated that all the plastic strains in the modelled parts are elastic; hence, the final product will exhibit a typical isotropic elasticity that most engineering materials exhibit, with the part returning to its original shape when the load is removed.

Figure 7 a–d show all the elastic strains of the component part. The elastic strain is a measure of the strain when the component is subjected to stresses beyond the yield point. The profile of the elastic strains are also seen to be identical, with most of the strains concentrated on the top surface close to the fixed point, but varying in magnitude as shown in the strain vs length plots for the three materials under consideration. The elastic strain distribution for the ABS material ranges between  $1.324 \times 10^{-8}$  and maximum value of  $3.337 \times 10^{-5}$ . For the epoxy material, its elastic strain distribution ranges between  $2.951 \times 10^{-9}$  and maximum value of  $7.438 \times 10^{-6}$ , while that of the Teflon ranges between  $1.248 \times 10^{-8}$  and maximum value of  $3.125 \times 10^{-5}$ . From the results, it can be concluded that the epoxy resin provides the best results, experiencing the least amount of strain followed by Teflon while ABS has the highest value of strain due to the stress induced under the required service condition.

The vertical deflections due to loading are presented in Fig. 8a–d. The deflections in the pictorial representations are magnified to give a clearer visualization of the change in the downward displacement of the product when loaded. Maximum deflections of between 0.00916 and 0.0411 mm were recorded which in real life may not be easily noticeable and as such it is insignificant to affect the functional requirement of the final product. The deflection distribution for the ABS material ranges between  $-4.112 \times 10^{-5}$  and maximum value of  $4.384 \times 10^{-8}$ . For the epoxy material, its deflection distribution ranges between  $-9.164 \times 10^{-6}$  and maximum value of  $9.77 \times 10^{-9}$ , while that of the Teflon ranges between  $-3.849 \times 10^{-5}$  and maximum value of  $4.103 \times 10^{-5}$ . The trend in the elastic strain results is reflected in the deflections, with the material with the least elastic strains (Resin) also showing the least downward deflection in response to the applied load, followed by Teflon and then ABS.

Figure 9 shows the interior of the printer before coupling while the coupled 3D printer developed for manufacturing. It was used for the manufacturing of the railcar accessory (fire extinguisher mount) shown in Fig. 10. The development of the machine had been reported earlier with recommendations for the optimization of the motion transmission mechanism and improvement in

the print efficiency. It was also recommended that the mechanical, thermal and surface roughness properties of printed materials be improved with the machine enabled to print different mix of materials in a single print operation [20]. It is in respect of this that the computer-aided simulation-based approach was employed for the determination of the mechanical properties of the three different print materials. The analysis of the results obtained showed that the developed product (fire extinguishing mount) possesses excellent strength that will ensure satisfactory rigidity under the required service conditions.

Although the additive manufacturing machine can be used for manufacturing other components for other applications. The scope of this work is limited to the development of a railcar accessory (fire extinguishing mount) and its performance evaluation.

In terms of the cost effectiveness, the manufacturing cost is a function of material employed, energy requirement and the printing time. The time of printing, however, depends on the part to be produced. The larger the size, the higher the production time and vice versa. This is because each of the layers produce often require substantial time to set before another one is added to it. In addition, components with dimensional irregularities or complex geometries will also require more printing time compared to the ones with simple shapes.

## 4 Conclusion

The computer-aided simulation and performance evaluation of a 3D printer were carried out in this study. The additive component manufacturing was limited to the railcar accessory (fire extinguishing mount). The modelling and simulation were carried out in the ABAQUS® 2016 environment. The performance evaluation carried out with the numerical and physical experimentations showed that the three printing materials evaluated, namely acrylonitrile butadiene styrene (ABS) plastic, epoxy resin and polytetrafluoroethylene have good mechanical properties that will ensure satisfactory strength under different loading conditions judging from the numerical analysis of the 3D printed models. The findings of this work provide a template for harnessing the prospects of additive manufacturing for high or low production in the manufacturing industry. Furthermore, it will also assist manufacturers in their quest for innovativeness in product development as well as reduction in the manufacturing lead time and cost. The production can be scaled using several physical models directly from the manufacturing digital data in ensuring a cost effective process and the development of a production process with rapid product development cycle.

## References

- Zhou C, Chen Y, Yang Z, Khoshnevis B (2013) Digital material fabrication using mask-image-projection-based stereolithography. *Rapid Prototyp J* 19(3):153–165
- Brooks BJ, Arif KM, Dirven S, Potgieter J (2017) Robot-assisted 3D printing of biopolymer thin shells. *Int J Adv Manuf Technol* 89(1–4):957–968
- Choi J-W, Kim H-C, Wicker R (2011) Multi-material stereolithography. *J Mater Process Technol* 211(3):318–328
- Gross BC, Erkal JL, Lockwood SY, Chen C, Spence DM (2014) Evaluation of 3D printing and its potential impact on biotechnology and the chemical sciences. *Anal Chem* 86(7):3240–3253
- Haigh JN, Dargaville TR, Dalton PD (2017) Additive manufacturing with polypropylene microfibers. *Mater Sci Eng C* 77:883–887
- Tymrak B, Kreiger M, Pearce JM (2014) Mechanical properties of components fabricated with open-source 3-D printers under realistic environmental conditions. *Mater Des* 58:242–246
- Manghnani R (2015) The impact of additive manufacturing on the automobile industry. *Int J Curr Eng Technol* 5(3):3407–3410
- Salea A, Prathumwan R, Junpha J, Subannajui K (2017) Metal oxide semiconductor 3D printing: preparation of copper (ii) oxide by fused deposition modelling for multi-functional semiconductor applications. *J Mater Chem C* 5(19):4614–4620
- Turner BN, Gold SA (2015) A review of melt extrusion additive manufacturing processes: materials, dimensional accuracy, and surface roughness. *Rapid Prototyp J* 21(3):250–261
- Vaezi M, Seitz H, Yang S (2013) A review on 3D micro-additive manufacturing technologies. *Int J Adv Manuf Technol* 67:1721–1754
- Deswal S, Narang R, Chhabra D (2019) Modeling and parametric optimization of FDM 3D printing process using hybrid techniques for enhancing dimensional preciseness. *Int J Interact Des Manuf* 13: 1197–1214
- Baechler C, DeVuono M, Pearce JM (2013) Distributed recycling of waste polymer into RepRap feedstock. *Rapid Prototyp J* 19(2): 118–125
- Liverani A, Caligiana G, Frizziero L, Francia D, Donnici G, Dhaimini K (2019) Design for six Sigma (DFSS) for additive manufacturing applied to an innovative multifunctional fan. *Int J Interact Des Manuf* 13:309–330
- Laplume A, Anzalone GC, Pearce JM (2016) Open-source, self-replicating 3-D printer factory for small-business manufacturing. *Int J Adv Manuf Technol* 85:633–642
- Valkenaers H, Vogeler F, Ferraris E, Voet A, Kruth JP (2013) A novel approach to additive manufacturing: screw extrusion 3D-printing. In: In: proceedings of the 10th international conference on multi-material micro manufacture, research publishing, pp 235–238
- Gurralla PK, Regalla SP (2014) Part strength evolution with bonding between filaments in fused deposition modelling. *Virtual Phys Prototyp* 9(3):141–149
- Wang J, Xie H, Weng Z, Senthil T, Wu L (2016) A novel approach to improve mechanical properties of parts fabricated by fused deposition modeling. *Mater Des* 105:152–159
- Chaidas D, Kitsakis K, Kechagias J, Maropoulos S (2016) The impact of temperature changing on surface roughness of FFF process. *IOP Conf Ser Mater Sci Eng* 161:012033 pp. 1–9
- Lužanin O, Movrin D, Plančak M (2013) Experimental investigation of extrusion speed and temperature effects on arithmetic mean surface roughness in FDM built specimens. *J Techn Plast* 38(2): 180–189
- Daniyan IA, Balogun V, Mpofu K, Omigbodun FT (2020) An interactive approach towards the development of an additive

- manufacturing technology for railcar manufacturing. *Int J Interact Des Manuf*. <https://doi.org/10.1007/s12008-020-00659-8>
21. MPDB, Material Properties Database Software Program (2019). Dassault Systèmes SolidWorks corporation, United States
  22. Bates-Green K, Howie T (2017) Materials for 3D printing by fused deposition. Edmonds Community College, pp 1–21
  23. Gibson I, Rosen DW, Stucker B (2010) Additive manufacturing technologies. Springer, New York
  24. Whyman S, Arif KM, Potgieter J (2018) Design and development of an extrusion system for 3D printing biopolymer pellets. *Int J Adv Manuf Technol* 96:3417–3428

**Publisher's note** Springer Nature remains neutral with regard to jurisdictional claims in published maps and institutional affiliations.